

# Metastable Zn-related centres in silicon

N T Bagraev

Ioffe Physico-Technical Institute, 26 Polytekhnicheskaya st.,  
St Petersburg 194021, Russia

Received 5 July 1993, in final form 13 October 1993, accepted for publication  
20 October 1993

**Abstract.** Photo-EPR evidence has yielded metastable negative- $U$  properties for Zn-related double acceptors in silicon. The spectral distributions of photoionization cross sections for  $D^-$  and  $D^{--}$  states of the orthorhombic Zn-related centre as well as the monoclinic CuZn and trigonal CrZn pairs are discussed. The data analysis in terms of a model for the deep defect tunnelling between the  $D_{2d}$  ( $D^0$  state),  $C_{2v}$  (paramagnetic  $D^-$  state) and  $C_{3v}$  ( $D^{--}$  state) interstitial lattice positions indicates that the  $(Zn_iV_{Si})^-$  orthorhombic centre should spontaneously decay into the  $(Zn_iV_{Si})^0$  and  $(Zn_iV_{Si})^{--}$  states, as is consistent with the negative- $U$  reaction:  $2D^- \rightarrow D^{--} + D^0$ , whereas the  $D^-$  state of the CuZn and CrZn pairs is more stable because of the energy barriers between the lattice positions of the centre charge states. A photo-EPR study of reactions involving the transfer of holes via the valence band between the orthorhombic Zn-related centres and CuZn pairs is also analysed. All aspects of the negative- $U$  properties for the orthorhombic Zn-related centre can be confirmed by monitoring the intensity of the EPR signals for Zn-related defects of both types.

## 1. Introduction

Zn-related defects are the best studied double acceptors in silicon [1–15]. Hall effect [1, 2], DLTS [3–5] and thermally induced capacitance [3] studies indicate that pairs of interrelated acceptor levels may be due to both single Zn centres and the complexes of Zn atoms with shallow acceptors and residual deep impurities. Microscopic models of Zn-related complexes are still lacking, while two centres, CuZn and CrZn, have been reported from EPR studies [7]. A general difficulty in the study of single Zn centres versus Zn-related complexes is that the ionization energies for the respective  $(0/-)$  and  $(-/-)$  acceptor levels are close in magnitude. This makes an unambiguous interpretation of optical data, e.g. from IR spectroscopy [10–13], virtually impossible and presents a major hindrance to finding a meaningful correlation with electrophysical results. Another difficulty is that Zn-related complexes and single Zn centres are usually present in comparable concentrations in the host silicon [4], which poses the problem of achieving reproducible performance characteristics in materials based on Zn-doped silicon, as used for example in IR detectors and charge-coupled devices [15].

In order to make sure that the electrophysical and optical data correspond to the target structural or compositional features in the Zn-related defect studied, it is desirable to employ combined magnetic resonance techniques, for example ODMR or photo-EPR. A benefit from the photo-EPR technique is the possibility of studying the relationship between the

electron–vibration interaction and charge correlations, and also the evolution of positive- $U$  to negative- $U$  transitions undergone by double acceptor electron levels in silicon.

It is the purpose of this paper to assess the capabilities of the photo-EPR method as a means of overcoming the above problems in the instance of the Si-NL36 orthorhombic Zn-related centre [7–9] as well as the Si-NL34 monoclinic CuZn and the Si-NL35 trigonal CrZn pairs [7].

We first discuss the spectral distributions of photoionization cross sections for the  $D^-$  and  $D^{--}$  states of three Zn-related centres, which were identified by the EPR method as the orthorhombic Zn-related centre [7–9] and the monoclinic CuZn and trigonal CrZn pairs [7]. These distributions were obtained from the time dependences of the regeneration and quenching for the respective photo-EPR signals. The paramagnetic  $D^-$  state of the orthorhombic Zn-related centre appeared only under optical pumping with monochromatic light. In the case of CuZn and CrZn pairs, the same conditions resulted in the quenching of the EPR signal from the stable  $D^-$  state that it has in the absence of illumination. To account for these observations, we further analyse the data in terms of the negative- $U$  reaction  $2D^- \rightarrow D^{--} + D^0$ , which can be suppressed in the presence of the energy barriers between the lattice positions of the  $D^0$ ,  $D^-$  and  $D^{--}$  states. We consider the short-range anisotropic Stark interaction as a metastability model of the negative- $U$  reaction in silicon containing Zn-related centres. Finally, the negative- $U$  properties for the orthorhombic Zn-related centre appear to be confirmed

by the photo-EPR results on the reactions involving the transfer of charge carriers between these centres and the CuZn pairs via the valence band.

## 2. Experiment

The host material was float-zone p-type silicon doped with boron to  $10^{13} \text{ cm}^{-3}$ . The diffusion of the  $^{67}\text{Zn}$  isotope was carried out in sealed quartz tubes at  $1200^\circ\text{C}$ . In order to ensure a uniform distribution of the zinc impurity, the diffusion process was allowed to run for periods of time up to 40 h. On completion of the diffusion step, the ampoules were quenched to room temperature. Subsequent preparation of the samples included polishing and etching. The total zinc concentration determined from the Hall effect measurements was about  $10^{16} \text{ cm}^{-3}$ .

The photo-EPR measurements were performed with an X-band EPR spectrometer using samples cooled to 4.2 K. Both the photo-EPR signal and the variations in its amplitude were induced by incandescent light; the monochromatic beam had access to the sample through a quartz window in the cryostat. The detected orthorhombic Zn-related centre, monoclinic CuZn and trigonal CrZn pairs were EPR identified [7–9] as NL36, NL34 and NL35 respectively (see figure 1). The CuZn and CrZn pairs resulted from the interaction of the zinc diffusant with the residual impurity; the interaction process could be controlled during the diffusion and subsequent thermal anneals. The Si-NL35 EPR spectrum was annealed at  $600^\circ\text{C}$ , while the concentrations of CuZn pairs and orthorhombic Zn-related centres appeared to increase with the thermal treatment [8, 9]. The fourfold splitting of the Si-NL36 EPR spectrum due to chromium hyperfine interaction and the kinetics of the annealing the Si-NL35 and Si-NL36 EPR spectra indicate that the Si-NL36 centre represents a distant orthorhombic donor–acceptor pair produced by the trigonal CrZn centre decay [9]. The metastable interrelation of the Si-NL35 and Si-NL36 centres is not, however, established, unlike the well-known metastable system of the orthorhombic and trigonal FeB pairs [16]. Moreover, since the presence of distant chromium in the Si-NL36 centre affects weakly the symmetry positions of the Zn charge states, this defect behaves like the orthorhombic single Zn centre in silicon.

## 3. Results

Double acceptors in silicon occur in their three charge states:  $\text{D}^0$ ,  $\text{D}^-$  and  $\text{D}^{--}$ , as pairs of interrelated levels,  $(0/-)$  and  $(-/-)$ , lying in the bandgap. Consequently, there is a possibility of studying these centres by monitoring the changes in the EPR signal amplitude caused by holes and electrons emitted from both levels under illumination with monochromatic light.

The amplitude variations of the EPR signal presented in figures 2, 3 and 4 demonstrate that the signal

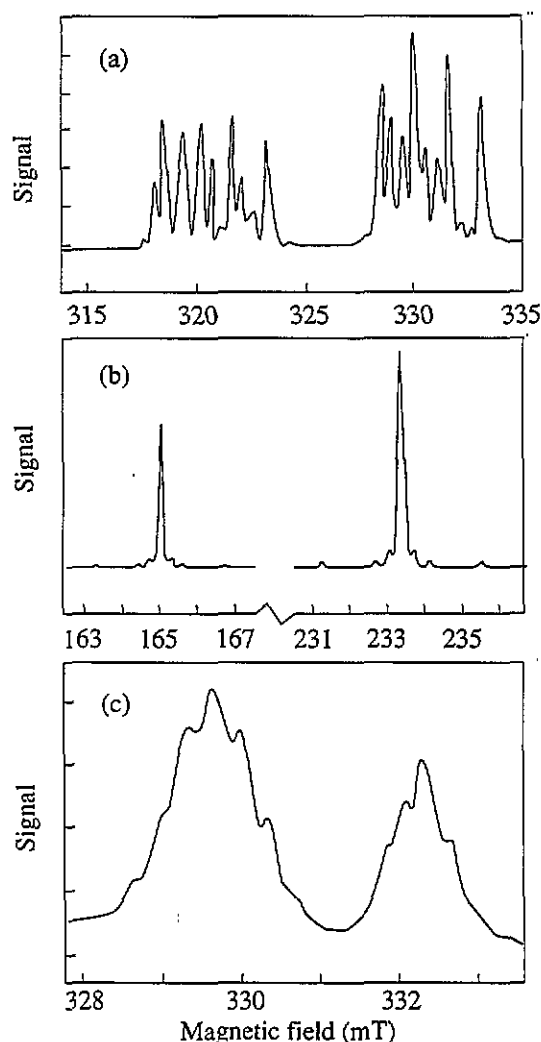


**Figure 1.** The EPR spectra of the Zn-related centres in p-type silicon [7–9].  $T = 4.2 \text{ K}$ ,  $\nu \approx 9 \text{ GHz}$ . (a) The monoclinic CuZn centre (Si-NL34),  $B \parallel [011]$ . (b) The trigonal CrZn centre (Si-NL35),  $B \parallel [011]$ . Fourfold splitting due to hyperfine interaction with the isotope  $^{53}\text{Cr}$ , 9.54%, natural abundance, is observable. (c) The orthorhombic Zn-related centre (Si-NL36),  $^{67}\text{Zn}$ ,  $B \parallel [100]$ . The EPR spectrum has been observed under illumination with monochromatic light,  $h\nu = 0.8 \text{ eV}$ .

experiences both quenching and regeneration. One can also get information on the spectral distribution of the photoionization cross sections for the  $\text{D}^-$  and  $\text{D}^{--}$  states of the monoclinic CuZn (figure 2) and trigonal CrZn (figure 3) pairs as well as the orthorhombic Zn-related centre (figure 4) in p-type silicon. Figures 2(a) and 3(a) show that the monoclinic and trigonal centres undergo a quenching phase followed by a regeneration event of very high  $h\nu$  selectivity. This suggests that the EPR quenching in the p-type silicon containing the CuZn ( $\text{Cu}^+\text{Zn}^-$ ) and CrZn ( $\text{Cr}^+\text{Zn}^-$ ) centres is apparently due to optical transitions from the valence band to the  $(-/-)$  level, i.e.  $\text{D}^- + h\nu \rightarrow \text{D}^{--} + h$ , and to the valence band from, for instance, the  $(0/-)$  level, i.e.  $(\text{D}^- + h) + h\nu \rightarrow \text{D}^0$ . On the contrary, the paramagnetic state of the orthorhombic centre is directly related to illumination, as is clear from figure 4(a). It is reasonable to suppose, therefore, that the paramagnetic  $\text{D}^-$  state of the orthorhombic Zn-related centre in p-type silicon

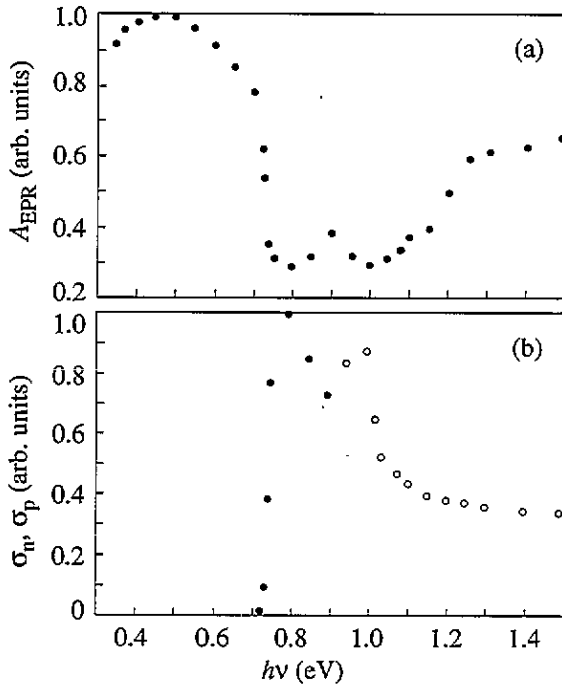


**Figure 2.** The monoclinic CuZn centre in p-type silicon. (a) Spectral dependence of quenching and regeneration of the Si-NL34 EPR spectrum. (b) Spectral dependences  $\sigma_n$  (○) and  $\sigma_p$  (●).

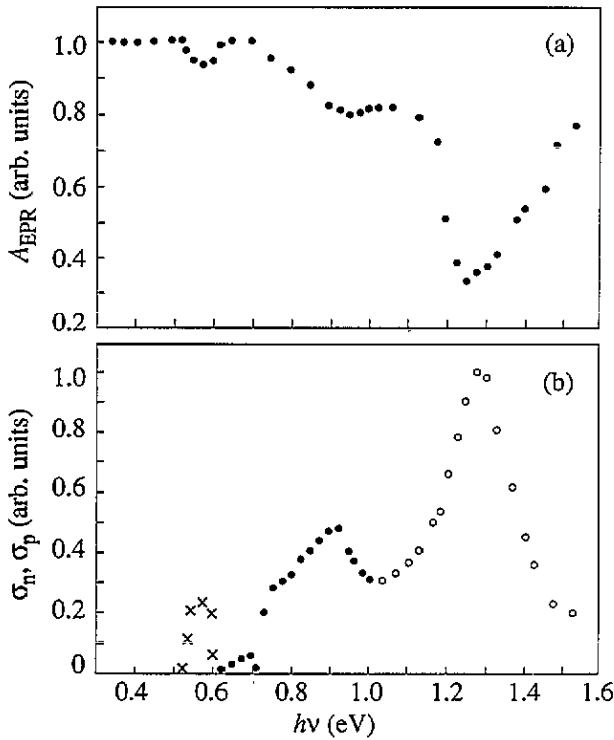


**Figure 3.** The trigonal CrZn centre in p-type silicon. (a) Spectral dependence of quenching and regeneration of the Si-NL35 EPR spectrum. (b) Spectral dependences  $\sigma_n$  (○),  $\sigma_p$  (●) and  $\sigma_{ch}$  (×).

results from the optical transitions that involve emission of a hole and creation of a  $(0/-)$  level,  $D^0 + h\nu \rightarrow D^- + h$ , or release of a hole to the valence band from, for instance, a  $(-/-)$  level,  $(D^{--} + h) + h\nu \rightarrow D^-$ .

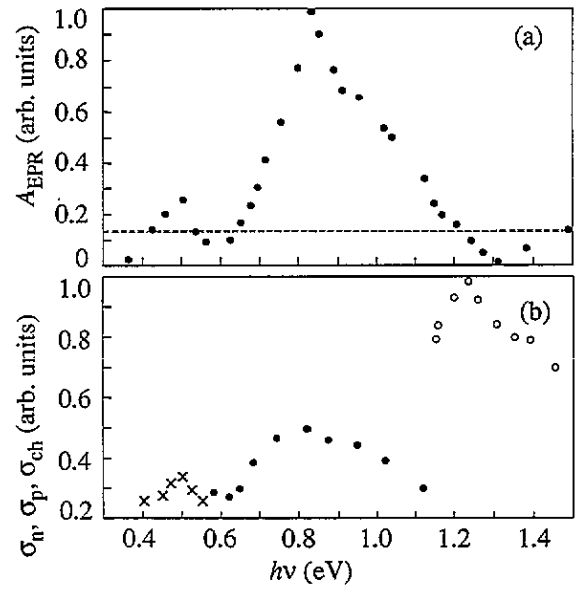


**Figure 4.** The orthorhombic Zn-related centre in p-type silicon. (a) Spectral dependence of quenching and regeneration of the Si-NL36 EPR spectrum. The broken line corresponds to the initial amplitude of the EPR spectrum after cooling of the sample. (b) Spectral dependences  $\sigma_n$  (○),  $\sigma_p$  (●) and  $\sigma_{ch}$  (×).

The photoionization cross sections for the  $D^-$  states

$$\sigma_{n1} \Rightarrow D^- + h\nu \rightarrow D^0 + e$$

$$\sigma_{p1} \Rightarrow D^0 + h\nu \rightarrow D^- + h$$

and  $D^{--}$  states

$$\sigma_{n2} \Rightarrow D^{--} + h\nu \rightarrow D^- + e$$

$$\sigma_{p2} \Rightarrow D^- + h\nu \rightarrow D^{--} + h$$

were determined from the time dependences of the EPR quenching and regeneration (figures 2(b), 3(b) and 4(b)). The good agreement between  $\sigma_n$ ,  $\sigma_p$  and the spectral dependences for the EPR signal amplitudes in figures 2(a), 3(a), 4(a) is a strong indication of the resonant nature of the  $D^0 \leftrightarrow D^-$  and  $D^- \leftrightarrow D^{--}$  optical transitions. The duration of the EPR quenching and regeneration was much less in the presence of optical pumping than without it, thus demonstrating the metastable character of the three Zn-related centres.

The spectral dependences in figures 2, 3 and 4 can be discussed using the two-electron adiabatic potential scheme presented in figure 5 [17–20]. Here the  $D^{--}$ ,  $D^-$  and  $D^0$  states are represented by the different positions of the double acceptor in the lattice because of the non-monotonic dependence of the electron–vibration constant on the charge state of a deep centre [18]. It should be noted that the use of two-electron adiabatic potentials (figure 5) demonstrates the difference between the energies of the optical and thermal transitions ( $D^0 \rightarrow D^-$  and  $D^- \rightarrow D^{--}$ ), while the equivalent one-electron band diagram (figure 6) would allow for the one-electron thermal transitions.

According to this scheme, the maxima (minima) on the spectral photo-EPR curves in p-type silicon

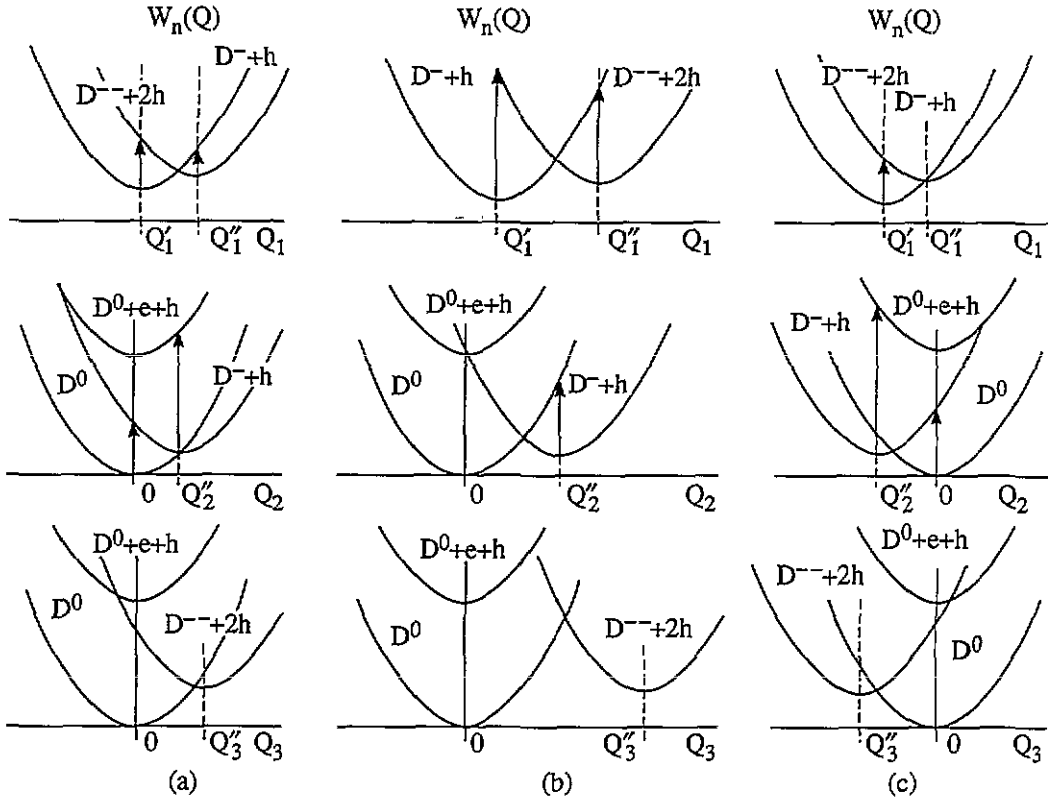


**Figure 5.** Two-electron adiabatic potentials for the monoclinic CuZn (a), trigonal CrZn (b) and orthorhombic (c) Zn-related centres in p-type silicon. Configuration coordinates  $Q_1$ ,  $Q_2$  and  $Q_3$  correspond to the directions in the Si lattice (see figures 8(a), (b) and (c)). The optical hole emission and the hole photocapture are marked by the arrows.

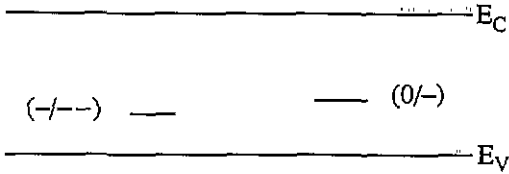
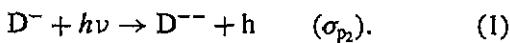
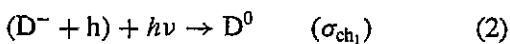


**Figure 6.** Equivalent one-electron band diagram for Zn centres in silicon, where the defect levels (0/-) and (-/-) display negative- $U$  ordering, according to the Hall energy measurements [19].

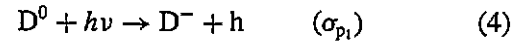
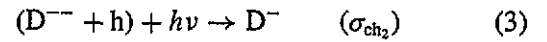
containing double acceptors can be related to the following processes:  $\sigma_{p1} \leftrightarrow \sigma_{n1}$  ( $D^0 + h\nu \rightarrow D^- + h$  and  $D^- + h\nu \rightarrow D^0 + e$ ),  $\sigma_{p2} \leftrightarrow \sigma_{ch2}$  ( $D^- + h\nu \rightarrow D^{--} + h$  and  $(D^{--} + h) + h\nu \rightarrow D^-$ ) and  $\sigma_{p1} \leftrightarrow \sigma_{ch1}$  ( $D^0 + h\nu \rightarrow D^- + h$  and  $(D^- + h) + h\nu \rightarrow D^0$ ). For example, the strong quenching of the EPR spectrum from the CrZn pair at  $h\nu = 0.9$  eV (figure 3) in p-type silicon may be attributed to the hole emission event that takes place at the paramagnetic  $D^-$  state of the  $Cr^+Zn^-$  centres (see figure 5(b)),



By the same logic, the quenching of the spectra that occurs at  $h\nu < 0.3$  eV (figure 2(a)) and 0.575 eV (figure 3(a)) may be due to the hole photocapture (figures 5(a) and 5(b) respectively),



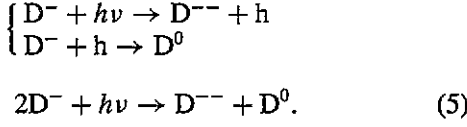
while their regeneration at 0.45 eV (figure 2(a)) and 0.67 eV (figure 3(a)) would be interpreted as a combined result of two reactions,



which are also illustrated in figures 5(a) and 5(b). In addition, the two-electron adiabatic potential scheme suggests that the broadening of the peaks in figures 2 and 3 may be due to the contribution made to the quenching and regeneration by phonon-assisted optical transitions.

It should be noted that the differences between the energies of the two-electron adiabatic potential minima in figure 5 represent the Hall energies for (0/-) and (-/-) transitions, which were determined for the three Zn-related centres investigated as  $E_V + 0.2$  eV and  $E_V + 0.17$  eV respectively, using the photo-Hall technique [19]. These results suggest that the Zn-related centres are negative- $U$  defects rather than ordinary double acceptors, with a paramagnetic  $D^-$  state that would readily dissociate into the  $D^{--}$  and  $D^0$  states, provided the sample were cooled. However, the paramagnetic  $D^-$  state of the  $Cu^+Zn^-$  and  $Cr^+Zn^-$  pairs is stable. The reason is again the metastable nature of the defect, which favours its 'freezing' in the  $D^-$  state. Figures 5(a) and 5(b) provide a plausible explanation of the causal relationship between the 'frozen' condition

of the one-electron state and the metastable nature of negative- $U$  defects in the form of the barriers separating the terms that belong to the  $D^{--}$  and  $D^-$  states. This obstacle to dissociation of the  $D^-$  state is removed, as figures 5(a) and (b) show, by the pumped light which gives rise to the above reactions (1) and (2):



The orthorhombic Zn-related centre, however, stands in sharp contrast with the monoclinic and trigonal centres in that virtually no EPR signal could be recorded in the absence of optical pumping. Illumination gives rise to a powerful EPR signal, as figure 4 amply testifies. Invoking again the two-electron adiabatic potential scheme, we can argue that the signal due to the absorption of 0.475 eV light is attributable to the production of the  $D^-$  paramagnetic state as a result of the  $(- - / -)$  optical transition (see equation (3)) that accompanies the photocapture of holes induced optically from the  $Cu^+Zn^-$  pairs (figures 2, 4 and 5(c)). The spectral minimum observed here for the photo-EPR signal at  $h\nu = 0.575$  eV (figure 4) must in turn be due to the  $D^- \rightarrow D^{--}$  optical transition (see equation (1) and figure 5(c)).

This behaviour of the double acceptor would seem to be nothing out of the ordinary but for two features. One is that a jump of the photo-EPR signal at  $h\nu > 0.6$  eV is at variance with the  $\sigma_{n_2} \ll \sigma_{p_2}$  relationship established for double acceptors in p-type silicon, and it would also be difficult to account for this jump in terms of the electron emission to the conduction band from the defects in the  $D^{--}$  state. In the light of the two-electron adiabatic potential scheme we suggest instead that the factor responsible for this effect is the enhancement of the emission of holes due to  $(0/-)$  optical transitions (see equation (4) and figures 4 and 5(c)). The other feature is of kinetic character: at  $0.525 \text{ eV} < h\nu < 0.575 \text{ eV}$  the photo-EPR signal first increases with the pumping time and then decreases to a value twice as large as its expected magnitude. The most satisfactory explanation for this observation would seem to be the metastability and negative- $U$  ordering as the inherent properties of acceptor levels arising from a competition between the hole photocapture,  $D^{--} \rightarrow D^-$  (equation (3)), and the hole photoemission,  $D^- \rightarrow D^{--}$  (equation (1)), which may be accompanied by hole Auger capture (see equations (1), (2) and (5) and figure 7(a)). Supporting evidence that the Auger reaction involving the  $D^-$  state does occur—in the form of spontaneous Auger dissociation (negative- $U$  reaction) [21–24], as it happens—is provided by double the quenching value observed for the photo-EPR signal on turning off the light ( $h\nu > 0.525$  eV) at the initial pumping stages (figure 7(b)):

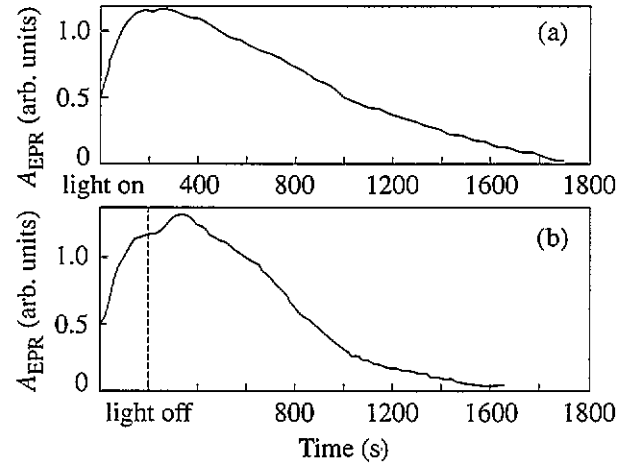
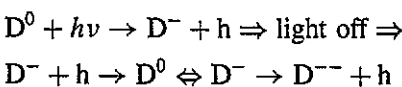
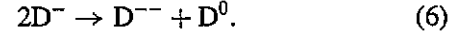


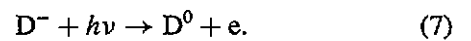
**Figure 7.** Time dependences for the photo-EPR (Si-NL36) signal. (a)  $h\nu = 0.525$  eV. (b)  $h\nu = 0.525$  eV plus subsequent relaxation with light off.



Apart from its academic value as an indication of the possible negative- $U$  properties for the orthorhombic Zn centre in p-type silicon, this result is a good check on the capabilities of the EPR technique. In fact, the sequence of reactions (1), (2), (5) and (6) provides an experimental test for the detection of negative- $U$  properties of defects in p-type semiconductors [17, 22]. The negative- $U$  properties for orthorhombic Zn centres in silicon have been confirmed by similar investigations in n-type silicon [19].

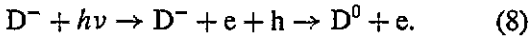
As pointed out earlier, there should be a correlation in the photoemission energies of holes and electrons involved in the reactions occurring on the  $D^-$  and  $D^{--}$  states (figure 5(c)). Indeed, the observations (figures 4 and 7) show a self-consistency between the regeneration and quenching spectra, thus confirming predictions of the photo-EPR behaviour from the adiabatic potential scheme of figure 5(c) [17, 18, 25]. Moreover, using this scheme (see figures 5(a) and 5(c)), it is possible to analyse the Auger processes involving the transfer of holes via the valence band between two different deep defects. For example, the quenching of the EPR spectrum from the  $CuZn$  pair at  $h\nu = 0.8$  eV (figure 2) may be attributed to the capture of additional holes due to  $(0/-)$  optical transitions (see equation (4)), which are responsible for the regeneration of the Si-NL36 centre at  $h\nu = 0.8$  eV (figure 4).

Illumination with light of higher energies has been observed to cause quenching of the EPR signal from both the  $Cu^+Zn^-$  ( $h\nu = 1.0$  eV) and  $Cr^+Zn^-$  ( $h\nu = 1.27$  eV) pairs as well as from the orthorhombic Zn-related centre ( $h\nu = 1.25$  eV) via a reaction apparently leading to excitation of electrons to the conduction band,



Since this reaction is more efficient than the emission of holes and electrons due to the interaction between the electron–vibration constant and charge correlations ( $\sigma_{n,2}$

and  $\sigma_{p_{1,2}}$ , see figure 5), we assume that the bandgap illumination can make a certain contribution to EPR quenching when high energy pumping light is used,



However, the fact that the spectral maxima  $\sigma_{n_1}$  for the three Zn-related centres differ in position on the curve provides a very strong argument in favour of reaction (7). Its leading role in the process is also indicated by the quantitative agreement between the energy associated with (7) and the energies required for the  $D^0 \leftrightarrow D^-$  and  $D^- \leftrightarrow D^{--}$  optical transitions, when one compares the corresponding plots in the configurational diagrams of figure 5. These summarize the photo-EPR results on the Zn-related centres (figures 2, 3 and 4) and can yield values for  $Q'_1 - Q''_1$ ,  $Q''_2$  and  $Q''_3$ —the configurational shifts (figure 5)—which are proportional to the separations between the lattice positions occupied by a deep centre in its different charge states, and hence may serve as a basis for a model of the reconstructed deep acceptor that we shall describe in the next section.

#### 4. Model

Figure 8 is a three-dimensional variant of figure 5 and shows that the fitting of the photo-EPR data (figures 2, 3 and 4) to the two-electron adiabatic potential scheme (figure 5) allows one to find the lattice positions of the centre charge states. This is because the scheme is capable of taking all of the coordinate directions into account [17, 26]. Indeed, the values of the configurational shifts  $Q'_1 - Q''_1$ ,  $Q''_2$  and  $Q''_3$  (figure 5), as determined from the EPR measurements for the orthorhombic Zn centre (figure 4), appear to be proportional to the separations between the  $C_{3v}$ ,  $C_{2v}$  and  $D_{2d}$  lattice positions. It then follows that the two-electron  $D^{--}$  state ( $n = 2$ ) can be modelled as the state of the centre located at the  $C_{3v}$  symmetry position [27,

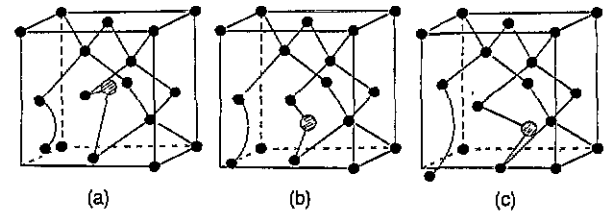


**Figure 9.** Model of a reconstructed double acceptor centre in silicon. (a)  $D^{--}$  state. (b)  $D^-$  state (orthorhombic Zn-related centre). (c)  $D^0$  state.

28], while the possible positions for the one-electron  $D^-$  state ( $n = 1$ ) and the empty  $D^0$  state ( $n = 0$ ) will be those corresponding to the  $C_{2v}$  and  $D_{2d}$  symmetries respectively (see figure 8(a)). The proposed layout of the positions for a reconstructed deep acceptor in its three states is illustrated in figure 9. Here parts (a) and (c) show, respectively, the  $C_{3v}$  and  $D_{2d}$  positions for the  $D^{--}$  and  $D^0$  states to which the orthorhombic Zn centre in its paramagnetic state, which is located at the position corresponding to  $C_{2v}$  symmetry (figure 9(b)), dissociates because of its negative- $U$  properties (via the reaction labelled as (6)). This layout helps one to visualize the tunnelling movements that the reconstructed defect will perform on changing its charge, a process caused by optical pumping [17, 28] between the above three symmetry positions by compensating for the Coulombic repulsion of electrons in the presence of a rigid lattice. It becomes clear from figures 2, 3 and 4 that the tunnelling movements are responsible for the reactions numbered (1)–(4) and (7), which lead to regeneration and quenching of the photo-EPR signal. It may be added that the  $C_{3v}$ – $C_{2v}$ – $D_{2d}$  triad of defect charge states has been proposed as a key to the understanding of the behaviour of oxygen thermodonors [29] and interstitial boron [30] in silicon.

When applied to the case of the  $Cu^+Zn^-$  and  $Cr^+Zn^-$  pairs, figures 8(b), 8(c) and 10 will show that the shifts experienced by the adiabatic potentials of the  $D^-$  and  $D^{--}$  states are due to the Stark effect in electric fields

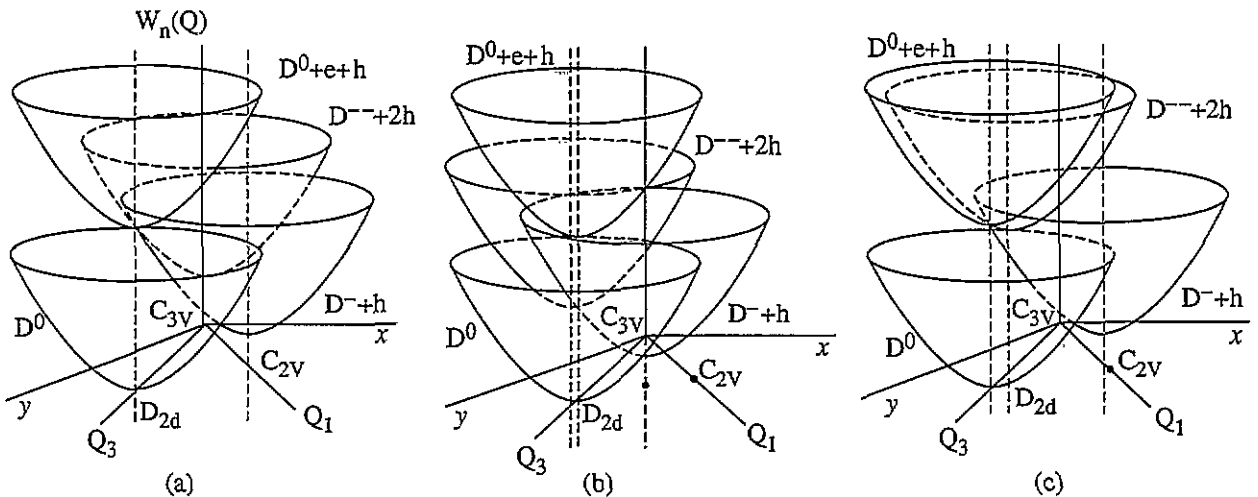


**Figure 8.** Three-dimensional two-electron adiabatic potentials for different charge states of the orthorhombic Zn-related (a), monoclinic CuZn (b) and trigonal CrZn (c) centres in p-type silicon. For the orthorhombic Zn-related centres the  $D^{--}$ ,  $D^-$  and  $D^0$  minima correspond, respectively, to the  $C_{3v}$ ,  $C_{2v}$  and  $D_{2d}$  symmetry lattice positions.

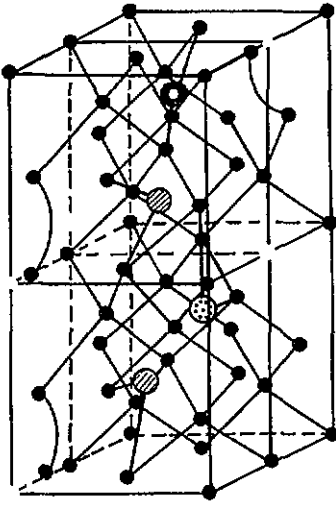


**Figure 10.** Model of reconstructed monoclinic  $\text{Cu}^+\text{Zn}^-$  and trigonal  $\text{Cr}^+\text{Zn}^-$  donor-acceptor pairs in the silicon lattice.  $\text{Zn}^-$  (striped circle),  $\text{Cu}^+$  (open circle) and  $\text{Cr}^+$  (textured circle).

induced in the presence of Cu and Cr donors near a Zn double acceptor [17, 28, 31]. The magnitudes of the shifts depend on the charge state of the centre and the angle at which the electric field  $E$  is inclined to the [110] and [111] crystallographic directions:

$$\begin{aligned} \delta Q'_1 &= (2eE/\kappa) \cos \Theta_1 & \Theta_1 &= [E \parallel [111]] \\ \delta Q'_2 &= (eE/\kappa) \cos \Theta_2 & \Theta_2 &= [E \parallel [110]] \end{aligned} \quad (9)$$

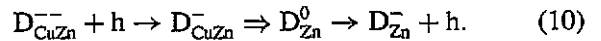
where  $\kappa$  is the force constant for the defect local vibration mode. By fitting the experimental values for  $Q'_1$ ,  $Q'_2$  (figures 2 and 3) and  $Q'_3$  (figures 5(a) and (b)) to the fixed separations between the  $\text{C}_{3V}$ ,  $\text{C}_{2V}$  and  $\text{D}_{2d}$  lattice positions, it is possible to determine the direction for the short-range anisotropic Stark interaction, and hence to establish the symmetry of a given defect. An example of such a fitting is given in figures 8(b), 8(c) and 10, where the axes of the  $\text{Cu}^+\text{Zn}^-$  and  $\text{Cr}^+\text{Zn}^-$  centres coincide with the direction of the internal electric field. This should be borne in mind when considering models for the CuZn monoclinic and CrZn trigonal centres (figure 10) that are based on the photo-EPR data obtained in the present work.

The two-electron adiabatic potential scheme also allows the optical and thermal ionization energies to be determined for the three types of Zn-related centre in silicon (figure 5). Two points should be emphasized regarding the energy values obtained.

The Stark effect can cause the potential to shift along  $Q$  even in the presence of relatively low external or internal electric fields ( $10^3$ – $10^6$  V cm $^{-1}$ ) and induce changes only in the optical and thermal values of the ionization energy, whereas the centre Hall energy of ionization, i.e. the difference between the adiabatic potential minima in figures 5(a) and (b), must remain constant (0.2 eV and 0.17 eV for (0/–) and (–/–) levels respectively). This explains why the formation of  $\text{Cu}^+\text{Zn}^-$  and  $\text{Cr}^+\text{Zn}^-$  pairs from an isolated Zn centre should be accompanied by suppression of the negative- $U$  reaction (6). The estimated value of 320 meV for

the optical transitions involving CuZn pairs appears to be in good agreement with numerous IR spectroscopic data [10–13] reported to date for Zn-related centres in silicon. The relevance of this agreement for the present discussion stems from our belief that most of the centres that have been detected with this technique (known to be incapable of identifying the recorded centre) are actually monoclinic CuZn pairs. These must almost invariably be present in Zn-doped silicon, having the concentrations that would normally, as our data indicate, exceed those of single centres by as much as an order of magnitude in both n- and p-type silicon.

We have also studied the transfer of holes and electrons between negative- $U$  centres with different metastabilities, which proceeds via the valence band with the light off. This type of reaction was first investigated by Watkins, who suggested the transfer to be evidence for the negative- $U$  properties of vacancies in silicon [22]. Figure 11 shows that photo-EPR signals from Si samples containing CuZn pairs and orthorhombic Zn centres display an antiphase behaviour immediately after the light is off. This 'overshoot' effect is due to Auger emission of electrons from the CuZn pair in the  $\text{D}^{--}$  state to the orthorhombic centre in the  $\text{D}^-$  state:



The hole transfer via the valence band leads to the growth of the EPR signal from the orthorhombic Zn centre and to the regeneration of the CuZn EPR spectrum. A small overshoot in figure 11 at the initial stage of the regeneration process probably arises from a fast capture of non-equilibrium holes at CuZn centres in the  $\text{D}^-$  state as a consequence of the low barrier between the one-electron state and the empty states (see figure 5(a) above). At the same time, the capture process is quickly suppressed by a far more powerful Auger reaction of the kind shown above as (10), so that the overshoot in the EPR signal from the CuZn pairs is very brief indeed when compared with a similar effect for an orthorhombic Zn-related centre. Later on, the signal from the CuZn pairs regenerates completely, while that

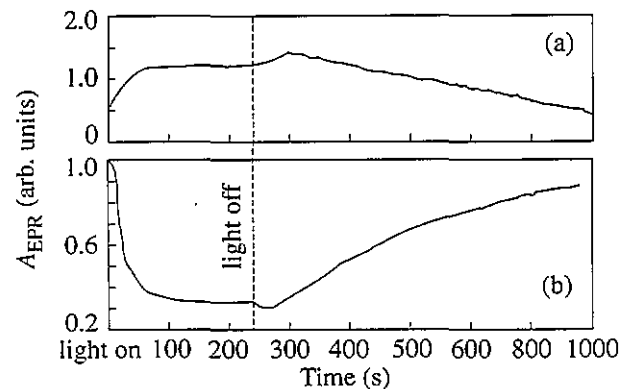


**Figure 11.** Time dependences for the photo-EPR signals.  $h\nu = 0.8$  eV plus subsequent relaxation with light off. (a) Si-NL36. (b) Si-NL34.

from the orthorhombic Zn centres experiences doubly strong quenching in their  $D^-$  states through a negative- $U$  reaction (6) stimulated by the Auger process.

Thus, the processes of quenching and regeneration of the EPR signal with the light off, which involve electron exchange via the valence band between the CuZn pairs and the orthorhombic Zn centres, confirm the metastable character of the negative- $U$  properties of these double acceptors.

## 5. Summary

Photo-EPR measurements have been employed to determine the spectral distributions of photoionization cross sections for different charge states of monoclinic CuZn (Si-NL34) and trigonal CrZn (Si-NL35) pairs as well as the orthorhombic Zn-related (Si-NL36) centres in silicon. The paramagnetic state of the orthorhombic Zn-related centre has been observed only under optical pumping, while the EPR spectra of the CuZn and CrZn pairs were found to be stable in the absence of illumination.

A model of deep double acceptor tunnelling between the  $D_{2d}$  ( $D^0$  state),  $C_{2v}$  (paramagnetic  $D^-$  state) and  $C_{3v}$  ( $D^{--}$  state) symmetry lattice positions has been proposed to account for the resonance nature of the  $D^0 \leftrightarrow D^-$  and  $D^- \leftrightarrow D^{--}$  optical transitions established from the spectral dependences of the photo-EPR signal. The results obtained—especially if viewed through this model—demonstrate different behaviour of the CuZn and CrZn pairs as well as the orthorhombic Zn-related centre under optical pumping in spite of the negative- $U$  ordering of the same Hall energies ( $(0/-) - E_V + 0.2$  eV and  $(-/-) - E_V + 0.17$  eV) for the three types of Zn-related centre. The  $D^-$  state of the orthorhombic Zn-related centre should spontaneously decay into the  $D^0$  and  $D^{--}$  states, as is consistent with the negative- $U$  reaction, and recover only after illumination with monochromatic light, whereas the  $D^-$  state of the CuZn and CrZn pairs is more stable because of the metastability displayed as the energy barriers between the lattice positions of the centre charge states. The photo-EPR data also point to the short-range anisotropic Stark interaction as the most probable cause of suppression of the negative- $U$  reaction involving the orthorhombic Zn-related centre in the transformation to the CuZn and CrZn pairs. The study of photo-induced reactions stimulating the exchange of non-equilibrium carriers via the valence band between the CuZn pairs and the orthorhombic Zn-related centres has confirmed the negative- $U$  properties of the latter defect.

## Acknowledgments

The author is grateful to H E Altink, T Gregorkiewicz and C A J Ammerlaan for helpful comments and experimental advice on the major part of this work, which was done during his sojourn at the Natuurkundig Laboratory, Amsterdam University.

## References

- [1] Fuller C S and Morin F J 1957 *Phys. Rev.* **105** 379
- [2] Carlson R C 1957 *Phys. Rev.* **108** 1390
- [3] Herman J M and Sah C T 1972 *Phys. Status Solidi a* **14** 405
- [4] Lemke H 1982 *Phys. Status Solidi a* **72** 177
- [5] Lebedev A A, Sultanov N A and Ecke W 1987 *Sov. Phys.-Semicond.* **21** 193
- [6] Yau L D and Sah C T 1971 *Phys. Status Solidi a* **6** 561
- [7] Altink H E, Gregorkiewicz T and Ammerlaan C A J 1990 *Solid State Commun.* **75** 115
- [8] Altink H E, Bagraev N T, Gregorkiewicz T and Ammerlaan C A J 1990 *Proc. XXth Int. Conf. on the Physics of Semiconductors* ed E M Anastassakis and J D Joannopoulos (Singapore: World Scientific) p 589
- [9] Altink H E 1993 *Thesis* Amsterdam University
- [10] Stolz P and Pensl G 1989 *Mater. Sci. Eng. B* **4** 31
- [11] Kornilov B V 1964 *Sov. Phys.-Solid State* **5** 2420
- [12] Merk E, Heyman J and Haller E E 1989 *Solid State Commun.* **72** 851
- [13] Dornen A, Kienle R, Thonke K, Stolz P, Pensl G, Grunebaum D and Stolwijk N A 1989 *Phys. Rev. B* **40** 1205
- [14] Weiss S, Beckman R and Kassing R 1990 *Appl. Phys. A* **50** 151
- [15] Sclar N 1977 *IEEE Trans. Electron Devices* **24** 709
- [16] van Kooten J J, Weller G A and Ammerlaan C A J 1984 *Phys. Rev. B* **30** 4564
- [17] Bagraev N T and Mashkov V A 1988 *Solid State Commun.* **65** 1111
- [18] Bagraev N T and Mashkov V A 1986 *Mater. Sci. Forum* **10-12** 435
- [19] Bagraev N T and Polovtsev I S 1993 *Defect and Diffusion Forum* **103-105** 345
- [20] Bagraev N T and Polovtsev I S 1992 *JETP Lett.* **56** 35
- [21] Anderson P W 1975 *Phys. Rev. Lett.* **34** 953
- [22] Watkins G D 1984 *Festkörperprobleme* **24** 163
- [23] Drabkin I A and Moizhes B Ya 1981 *Sov. Phys.-Semicond.* **15** 357
- [24] Alt H Ch 1992 *Mater. Sci. Forum* **83-87** 369
- [25] Baraff G A 1986 *Mater. Sci. Forum* **10-12** 377
- [26] Itoh N 1985 *Defects in Semiconductors* vol 14a, ed L C Kimerling and J M Parsey Jr (New York: Metal Soc.) 31
- [27] Morgan T N 1989 *Mater. Sci. Forum* **38-41** 1079
- [28] Bagraev N T 1991 *J. Physique* **1** 1511
- [29] Benton J L, Lee K M, Freeland P E and Kimerling L C 1985 *Defects in Semiconductors* vol 14a, ed L C Kimerling and J M Parsey Jr (New York: Metal Soc.) p 647
- [30] Watkins G D 1987 *Phys. Rev. B* **36** 1094
- [31] Dobaczewski L 1989 *Mater. Sci. Forum* **38-41** 113